

SPATIAL FILTRATION OF SHEAR INTERFEROGRAMS DURING HOLOGRAPHIC INTERFEROMETRY OF A FOCUSED IMAGE

V.G. Gusev

V.V. Kuibyshev State University, Tomsk

Received February 15, 1990

Analysis of the double exposure technique for recording holograms of a focused image of a mat screen is presented. The technique enables one to obtain shear interferograms. It is shown both theoretically and experimentally, that spatial filtration in the corresponding planes allows one to filter either the shear interferogram characterizing the phase distortions of the wave illuminating the mat screen and of the reference wave, or the shear interferogram characterizing the wave aberrations of the lens used to record the hologram.

In Ref. 1 I demonstrated that a doubly exposed lens-free Fourier hologram produced by a diffusely scattered radiation field may yield a shear interferogram for the quality control of a spherical wavefront.

The present article considers a technique of double-exposure recording of the hologram of a focused image for the quality control of lenses and objectives by their image field. The recording scheme is shown in Fig. 1. A mat screen 1 positioned in the plane (x_1, y_1) is illuminated by a coherent plane wave incident normal to its surface. The lens L_1 forms a hologram recording of the focused image of that screen on the photographic plate 2 projecting the off-axis plane wave 3. This recording takes place during the first exposure of the plate. In the Fresnel approximation, neglecting the amplitude and phase factors, which remain constant in any plane, the complex field amplitude in the plane (x_3, y_3) of the photometric plate takes the following from:

$$u_1(x_3, y_3) \sim \int_{-\infty}^{\infty} \int_{-\infty}^{\infty} \int_{-\infty}^{\infty} t(x_1, y_1) \exp i\varphi_1(x_1, y_1) \times$$

$$\begin{aligned} & \times \exp\left\{ \frac{ik}{2l_1} \left[(x_1 - x_2)^2 + (y_1 - y_2)^2 \right] \right\} p_1(x_2, y_2) \times \\ & \times \exp i\varphi_2(x_2, y_2) \exp\left[-\frac{ik}{2f_1} (x_2^2 + y_2^2) \right] \times \\ & \times \exp\left\{ \frac{ik}{2l_2} \left[(x_2 - x_3)^2 + (y_2 - y_3)^2 \right] \right\} dx_1 dy_1 dx_2 dy_2, \end{aligned} \quad (1)$$

where k is the wave number; $t(x_1, y_1)$ is the complex transmittance of the mat screen, which is a random function of the running coordinates; $\varphi(x_1, y_1)$ is the phase function which characterizes the illuminating wavefront distortions due to aberrations in the optical system forming it; $p_1(x_2, y_2)\exp i\varphi_2(x_2, y_2)$ is the generalized pupil function of the lens L_1 (focal distance f_1 , (see Ref. 2) which accounts for its axial wave aberrations; l_1 and l_2 are, respectively, the distance between the planes (x_1, y_1) , (x_2, y_2) and (x_2, y_2) , (x_3, y_3) .

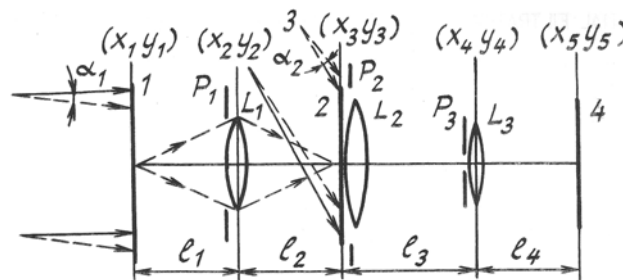


FIG. 1. Optical diagram of recording and recovery of the doubly exposed hologram of a focused image: 1) mat screen; 2) photographic-plate-hologram; 3) reference beam; 4) interferogram recording plane; L_1, L_2, L_3 — lenses; p_1, p_2, p_3 — aperture diaphragms.

Since $1/f_1 = 1/l_1 + 1/l_2$, expression (1) may be transformed to yield

$$u_1(x_3, y_3) \sim \left[\frac{ik}{2l_2} (x_3^2 + y_3^2) \right] \left\{ t[-\mu_1 x_3, -\mu_1 y_3] \times$$

$$\begin{aligned} & \times \exp i\varphi_1[-\mu_1 x_3, -\mu_1 y_3] \exp i \left[\frac{k\mu_1^2}{2l_1} (x_3^2 + y_3^2) \right] \otimes \\ & \otimes P_1(x_3, y_3) \left. \right\}, \end{aligned} \quad (2)$$

where $\mu_1 = l_1/l_2$ is the scale factor, and \otimes denotes the operation of convolution;

$$P_1(x_3, y_3) = \iint_{-\infty}^{\infty} p_1(x_2, y_2) \exp i\varphi_2(x_2, y_2) \times \exp \left[-\frac{ik}{l_2} (x_2x_3 + y_2y_3) \right] dx_2 dy_2$$

is the Fourier transform of the generalized pupil function of the lens L_1 . If, prior the second exposure, the tilt angle of the incident wavefront is changed by α_1 in the (x, z) plane, and the tilt angle of the reference wavefront in the same plane is changed by α_2 , then the complex amplitude of the object field in the plane of the photographic plate, corresponding to the second exposure, is given by the expression

$$u_2(x_3, y_3) \sim \exp \left[\frac{ik}{2l_2} (x_3^2 + y_3^2) \right] \left\{ t(-\mu_1x_3, -\mu_1y_3) \times \exp i\varphi_1(-\mu_1x_3 + a, -\mu_1y_3) \exp i[-ik\mu_1x_3 \sin\alpha_1] \times \exp \left[\frac{ik\mu_1^2}{2l_1} (x_3^2 + y_3^2) \right] \otimes P_1(x_3, y_3) \right\}, \quad (3)$$

where a is the shift due to the change in the incident wavefront tilt prior to the second exposure. We represent the distribution of the complex amplitude of the reference field in the plane of the photographic plate as $u_{01} \sim \exp i[kx_3 \sin\theta + \varphi_3(x_3, y_3)]$, where θ is its angle of incidence on the photographic plate; $\varphi_3(x_3, y_3)$ is the phase function characterizing the distortions of the reference wavefront due to aberrations in the optical system forming it. During the second exposure the complex amplitude of the reference wave at the photographic plate may then be expressed as $u_{02} \sim \exp i[kx_3 \sin(\theta - \alpha_2) + \varphi_3(x_3 - b, y_3)]$, where b is the shift due to the change of the reference wavefront tilt prior to the second exposure.

Let such a doubly exposed hologram of the focused image of the mat screen be recovered by a copy of the reference wave with complex amplitude distribution u_{01} . Assuming that the lens L_1 (see Fig. 1) is positioned in the hologram plane, the complex amplitude of the diffraction field in the (x_4, y_4) plane in the "minus first" diffraction order is given by the expression

$$u(x_4, y_4) \sim \iint_{-\infty}^{\infty} \left\{ u_1(x_3, y_3) + u_2(x_3, y_3) \times \exp i \left\{ kx_3 [\sin\theta - \sin(\theta - \alpha_2)] + \varphi_3(x_3, y_3) - \varphi_3(x_3 - b, y_3) \right\} \right\} p_2(x_3, y_3) \exp \left[-\frac{ik}{2f_2} (x_3^2 + y_3^2) \right] \times$$

$$\times \exp \left\{ \frac{ik}{2l_3} [(x_3 - x_4)^2 + (y_3 - y_4)^2] \right\} dx_3 dy_3, \quad (4)$$

where f_2 is the focal distance of the lens L_2 with pupil function $p_2(x_3, y_3)$, whose diameter depends on the size of the image of the mat screen; and t_3 is the distance between the (x_3, y_3) and (x_4, y_4) planes.

Upon substituting expressions (2) and (3) into expression (4), assuming that the conditions $1/f_2 = 1/l_2 + 1/l_3$ and $\sin\theta - \sin(\theta - \alpha_2) = \mu_1 \sin\alpha_1$ are satisfied, we obtain

$$u(x_4, y_4) \sim \exp \left[\frac{ik}{2l_3} (x_4^2 + y_4^2) \right] \left\{ F \left[\frac{kx_4}{l_3}, \frac{ky_4}{l_3} \right] \times p_1(-\mu_2x_4, -\mu_2y_4) \exp i\varphi_2(-\mu_2x_4, -\mu_2y_4) \otimes P_2(x_4, y_4) + F \left[\frac{kx_4}{l_3}, \frac{ky_4}{l_3} \right] \times p_1(-\mu_2x_4 + \alpha_2 l_2 \cos\theta, -\mu_2y_4) \times \exp i\varphi_2(-\mu_2x_4 + \alpha_2 l_2 \cos\theta, -\mu_2y_4) \otimes \Phi_1(x_4, y_4) \otimes \Phi_2(x_4, y_4) \otimes P_2(x_4, y_4) \right\}. \quad (5)$$

To simplify these expressions, we assume below that $\mu_1\alpha_1 = \alpha_2 \cos\theta$ for small angles. In Eq. (5) $\mu_2 = l_2/l_3$ is the scale factor. The expressions

$$F \left[\frac{kx_4}{l_3}, \frac{ky_4}{l_3} \right] = \iint_{-\infty}^{\infty} t(-\mu_1x_3, -\mu_1y_3) \times \exp i\varphi_1(-\mu_1x_3, -\mu_1y_3) \exp i \left[\frac{k\mu_1^2}{2l_1} (x_3^2 + y_3^2) \right] \times \exp \left[-\frac{ik}{2l_3} (x_3x_4 + y_3y_4) \right] dx_3 dy_3;$$

$$P_2(x_4, y_4) = \iint_{-\infty}^{\infty} p_2(x_3, y_3) \times \exp \left[-\frac{ik}{l_3} (x_3x_4 + y_3y_4) \right] dx_3 dy_3;$$

$$\Phi_1(x_4, y_4) = \iint_{-\infty}^{\infty} \exp i \left[\varphi_1(-\mu_1x_3 + a, -\mu_1y_3) - \varphi_1(-\mu_1x_3, -\mu_1y_3) \right] \exp \left[-\frac{ik}{l_3} (x_3x_4 + y_3y_4) \right] dx_3 dy_3;$$

$$\Phi_2(x_4, y_4) = \iint_{-\infty}^{\infty} \exp i \left[\varphi_3(x_3, y_3) - \varphi_3(x_3 - b, y_3) \right] \times$$

$$\times \exp\left[-\frac{ik}{l_3}(x_3x_4 + y_3y_4)\right] dx_3 dy_3$$

are the Fourier transforms of the corresponding functions.

As follows from Eq. (5), if the width of the function $\Phi_1(x_4, y_4) \otimes \Phi_2(x_4, y_4)$ is much less than that of the function $P_2(x_4, y_4)$ (the latter determines the speckle size in the (x_4, y_4) plane), then the speckle fields of the two exposures coincide within the overlapping images of the pupil of lens L_1 . Hence, as follows from Ref. 3, the interference pattern which, according to Eq. (5), characterizes the wave aberrations produced by the lens L_1 , is localized in the (x_4, y_4) plane. Let the lens L_3 be positioned in the (x_4, y_4) plane. Then the complex amplitude of the diffracted field in the detection plane 4 (see Fig. 1) is given by

$$u(x_5, y_5) \sim \iint_{-\infty}^{\infty} u(x_4, y_4) p_3(x_4, y_4) \times \exp\left[-\frac{ik}{2f_3}(x_4^2 + y_4^2)\right] \times \exp\left\{\frac{ik}{2l_4}[(x_4 - x_5)^2 + (y_4 - y_5)^2]\right\} dx_4 dy_4, \quad (6)$$

where f_3 is the focal distance of the lens L_3 with pupil function $P_3(x_4, y_4)$, and l_4 is the distance between (x_4, y_4) and (x_5, y_5) planes.

Substituting expression (5) into expression (6), we assume that the condition $\varphi_2(-\mu_1x_4 + \alpha_2l_2\cos\theta, -\mu_2y_4) - \varphi_2(-\mu_2x_4, -\mu_2y_4) \leq \pi$ is satisfied within the pupil diameter of lens L_3 . The latter condition corresponds to correlated speckle fields in the space between the planes (x_4, y_4) and (x_5, y_5) . In addition, the following equality is satisfied: $1/f_3 = 1/l_3 + 1/l_4$. We then obtain

$$u(x_5, y_5) \sim \exp\left[\frac{ik}{2l_4}(x_5^2 + y_5^2)\right] \left\{ t(\mu_1\mu_3x_5, \mu_1\mu_3y_5) \times \exp i\varphi_1(\mu_1\mu_3x_5, \mu_1\mu_3y_5) \exp i\left[\frac{k\mu_1^2\mu_3^2}{2l_1}(x_5^2 + y_5^2)\right] \otimes P_3(x_5, y_5) + t(\mu_1\mu_3x_5, \mu_1\mu_3y_5) \times \exp i\varphi_1(\mu_1\mu_3x_5 + \alpha, \mu_1\mu_3y_5) \exp i\left[\varphi_3(-\mu_3x_5, -\mu_3y_5) - \varphi_3(-\mu_3x_5 - b, -\mu_3y_5)\right] \otimes P_3(x_5, y_5) \right\}, \quad (7)$$

where $\mu_3 = l_3/l_4$ is the scale factor, and

$$P_3(x_5, y_5) = \iint_{-\infty}^{\infty} p_3(x_4, y_4) \times \exp\left[-\frac{ik}{l_4}(x_4x_5 + y_4y_5)\right] dx_4 dy_4$$

is the Fourier transform of the lens L_3 pupil function.

As follows from Eq. (7), the correlated speckle fields of the two exposures coincide in the (x_5, y_5) plane. If the width of the function $P_3(x_5, y_5)$, which determines the size of an individual speckle in the detection plane 4 (see Fig. 1) is at least an order of magnitude less than the period of the function

$$\exp i\left[\varphi_3(-\mu_3x_5, -\mu_3y_5) - \varphi_3(-\mu_3x_5 - b, -\mu_3y_5) + \varphi_1(\mu_1\mu_3x_5 + \alpha, \mu_1\mu_3y_5) - \varphi_1(\mu_1\mu_3x_5, \mu_1\mu_3y_5)\right]$$

(see Ref. 4), then that function can be taken outside the convolution integral in expression (7). The irradiance distribution in the (x_5, y_5) plane is then given by

$$I(x_5, y_5) \sim \left\{ 1 + \cos\left[\varphi_3(-\mu_3x_5, -\mu_3y_5) - \varphi_3(-\mu_3x_5 - b, -\mu_3y_5) + \varphi_1(\mu_1\mu_3x_5 + \alpha, \mu_1\mu_3y_5) - \varphi_1(\mu_1\mu_3x_5, \mu_1\mu_3y_5)\right] \right\} \left| t(\mu_1\mu_3x_5, \mu_1\mu_3y_5) \times \exp\left[\frac{ik\mu_1^2\mu_3^2}{2l_1}(x_5^2 + y_5^2)\right] \otimes P_3(x_5, y_5) \right|^2, \quad (8)$$

which describes the speckle structure modulated by the interference bands. The interference pattern is essentially the shear interferogram in the bands of infinite width. It characterizes the phase distortions of the wave illuminating the mat screen and of the reference wave. Such distortions appear in the image due to wave aberrations in the optical systems forming these waves. It follows from the above analysis that the interference pattern is localized in the hologram plane, so that to record it spatial filtration is needed in the image plane of the pupil of lens L_1 . In addition, because of the presence of phase factor characterizing the distribution of the complex amplitude of a divergent spherical wave of a curvature radius 1 in expressions (2) and (3), a collimating lens L is needed in the hologram plane to record the interference pattern in the minus first diffraction order. Such a lens becomes unnecessary if we record another shear hologram, characterizing the distortions of the illuminating wavefront and of the reference wavefront in the plus first order of diffraction. Indeed, according to Fig. 2 the diffraction field in the plus first diffraction order in the plane (x_4, y_4) , a distance l_2 from the hologram, takes the form

$$u'(x_4, y_4) \sim \exp\left[\frac{ik}{2l_2}(x_4^2 + y_4^2)\right] \left\{ F' \left[\frac{kx_4}{l_2}, \frac{ky_4}{l_2} \right] \times p_1(x_4, y_4) \exp i\varphi_2(x_4, y_4) \otimes P_2(x_4, y_4) + F' \left[\frac{kx_4}{l_2}, \frac{ky_4}{l_2} \right] p_1(x_4 + \alpha_2l_2\cos\theta, y_4) \times \right.$$

$$\times \exp[-i\varphi_2(x_4 + \alpha_2 l_2 \cos\theta, y_4)] \otimes \Phi'_1(x_4, y_4) \otimes \Phi'_2(x_4, y_4) \otimes P'_2(x_4, y_4) \Big\}, \tag{9}$$

where

$$F' \left[\frac{kx_4}{l_2}, \frac{ky_4}{l_2} \right] = \iint_{-\infty}^{\infty} t^* (-\mu_1 x_3, -\mu_1 y_3) \times \exp[-i\varphi_1(-\mu_1 x_3, -\mu_1 y_3)] \exp \left[-\frac{ik\mu_1^2}{2l_1} (x_3^2 + y_3^2) \right] \times \exp \left[-\frac{ik}{l_2} (x_3 x_4 + y_3 y_4) \right] dx_3 dy_3,$$

$$P'_2(x_4, y_4) = \iint_{-\infty}^{\infty} p_2(x_3, y_3) \times \exp \left[-\frac{ik}{l_2} (x_3 x_4 + y_3 y_4) \right] dx_3 dy_3,$$

$$\Phi'_1(x_4, y_4) = \iint_{-\infty}^{\infty} \exp i \left[\varphi_1(-\mu_1 x_3, -\mu_1 y_3) - \varphi_1(-\mu_1 x_3 + a, -\mu_1 y_3) \right] \times \exp \left[-\frac{ik}{l_2} (x_3 x_4 + y_3 y_4) \right] dx_3 dy_3,$$

$$\Phi'_2(x_4, y_4) = \iint_{-\infty}^{\infty} \exp i \left[\varphi_3(x_3 - b, y_3) - \varphi_3(x_3, y_3) \right] \times \exp \left[-\frac{ik}{l_2} (x_3 x_4 + y_3 y_4) \right] dx_3 dy_3$$

are the Fourier transforms of the corresponding functions.

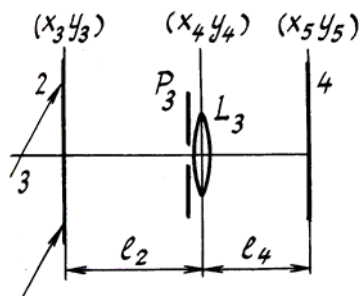


FIG. 2. Spatial filtration of the light field of a doubly exposed hologram in the plus-first order of diffraction in the image plane of the pupil of lens L_1 .

As follows from Eq. (9), the speckle fields of the two exposures coincide within the overlapping images of the pupil of lens L_1 . Hence the interference pattern

characterizing the wave aberrations due to lens L_1 is localized in that plane. If the lens L_3 is positioned in the same plane (see Fig. 2) the complex amplitude of the diffraction field in the detection plane 4 can be determined from Eq. (6). Substituting expression (9) into expression (6), we must satisfy the equality $1/f_3 = 1/l_2 + 1/l_4$, and within the pupil diameter of lens L_3 , the inequality $\varphi_2(x_4 + \alpha_2 l_2 \cos\theta, y_4) - \varphi_2(x_4, y_4) \leq \pi$, i.e., the pupil diameter of lens L_3 should not exceed the interference bandwidth for the interference pattern localized in the plane (x_4, y_4) . These conditions lead to the following distribution of the diffraction field in the detection plane 4

$$u'(x_5, y_5) \sim \exp \left[\frac{ik}{2l_4} (x_5^2 + y_5^2) \right] \left\{ t^* (\mu_1 \mu'_3 x_5, \mu_1 \mu'_3 y_5) \times \exp[-i\varphi_1(\mu_1 \mu'_3 x_5, \mu_1 \mu'_3 y_5)] \times \exp \left[-\frac{ik\mu_1^2 \mu_3'^2}{2l_1} (x_5^2 + y_5^2) \right] \otimes P_3(x_5, y_5) + t^* (\mu_1 \mu'_3 x_5, \mu_1 \mu'_3 y_5) \exp[-i\varphi_1(\mu_1 \mu'_3 x_5 + a, \mu_1 \mu'_3 y_5)] \times \exp i \left[\varphi_3(-\mu'_3 x_5 - b, -\mu'_3 y_5) - \varphi_3(-\mu'_3 x_5, -\mu'_3 y_5) \right] \times \exp \left[-\frac{ik\mu_1^2 \mu_3'^2}{2l_1} (x_5^2 + y_5^2) \right] \otimes P_3(x_5, y_5) \right\}, \tag{10}$$

where $\mu'_3 = l_2 / l_4$ is the scale factor.

Assuming that the size of the speckle in the detection plane 4 is small in comparison with the period at which the speckle field phase is modulated, we obtain from Eq. (10) the irradiance distribution in the plane (x_5, y_5)

$$I'(x_5, y_5) \sim \left\{ 1 + \cos \left[\varphi_3(-\mu'_3 x_5 - b, -\mu'_3 y_5) - \varphi_3(-\mu'_3 x_5, -\mu'_3 y_5) + \varphi_1(\mu_1 \mu'_3 x_5, \mu_1 \mu'_3 y_5) - \varphi_1(\mu_1 \mu'_3 x_5 + a, \mu_1 \mu'_3 y_5) \right] \right\} \left| t^* (\mu_1 \mu'_3 x_5, \mu_1 \mu'_3 y_5) \times \exp \left[-\frac{ik\mu_1^2 \mu_3'^2}{2l_1} (x_5^2 + y_5^2) \right] \otimes P_3(x_5, y_5) \right|^2, \tag{11}$$

From expressions (8) and (11) it follows that if one disregards the difference in the scales of the transformations, then the form of the interference patterns given by expressions (8) and (11) is identical, with the exception that the irradiance distributions they describe are 180° out of phase.

Let a doubly exposed hologram be reproduced by a copy of the reference wave with complex amplitude distributed according to u_{01} . Let also the diffraction

field be spatially filtered in accordance with Fig. 3, on the optical axis in the hologram plane with the help of the aperture diaphragm of lens L_2 . Then the complex amplitude of the diffraction field immediately behind the diaphragm take the form

$$\begin{aligned}
 u(x_3, y_3) &\sim p_2(x_3, y_3) \exp\left[\frac{ik}{2l_2}(x_3^2 + y_3^2)\right] \times \\
 &\times \left\{ t(-\mu_1 x_3, -\mu_1 y_3) \exp i\varphi_1(-\mu_1 x_3, -\mu_1 y_3) \times \right. \\
 &\times \exp i\left[\frac{k\mu_1^2}{2l_1}(x_3^2 + y_3^2)\right] \otimes P_1(x_3, y_3) + \\
 &+ \left. \left\{ t(-\mu_1 x_3, -\mu_1 y_3) \exp i\varphi_1(-\mu_1 x_3 + a, -\mu_1 y_3) \times \right. \right. \\
 &\times \left. \left. \exp[-ik\mu_1 x_3 a] \exp i\left[\frac{k\mu_1^2}{2l_1}(x_3^2 + y_3^2)\right] \otimes P_1(x_3, y_3) \right\} \times \right. \\
 &\times \left. \exp i\left[kx_3 a_2 \cos\theta + \varphi_3(x_3, y_3) - \varphi_3(x_3 - b, y_3)\right] \right\}. \quad (12)
 \end{aligned}$$

We may take the function $\exp i[\varphi_1(-\mu_1 x_3 + a, -\mu_1 y_3) - \varphi_1(-\mu_1 x_3, -\mu_1 y_3)]$ out from inside the convolution integral in expression (12), assuming that its period of variation is much longer than that of the speckle in the plane (x_3, y_3) (the latter is determined by the width of the function $P_1(x_3, y_3)$). If within the diameter of the aperture diaphragm P_2 the inequality $\varphi_1(-\mu_1 x_3 + a, -\mu_1 y_3) - \varphi_1(-\mu_1 x_3, -\mu_1 y_3) + \varphi_3(x_3, y_3) - \varphi_3(x_3 - b, y_3) \leq \pi$ is satisfied, then, assuming that the condition $1/f_2 = 1/l_2 + 1/l_3$ is satisfied, the complex amplitude of the diffraction field in the plane (x_4, y_4) is given by the expression

$$\begin{aligned}
 u(x_4, y_4) &\sim \exp\left[\frac{ik}{2l_3}(x_4^2 + y_4^2)\right] \left\{ F\left[\frac{kx_4}{l_3}, \frac{ky_4}{l_3}\right] \times \right. \\
 &\times p_1(-\mu_2 x_4, -\mu_2 y_4) \exp i\varphi_2(-\mu_2 x_4, -\mu_2 y_4) \otimes P_2(x_4, y_4) + \\
 &+ F\left[\frac{kx_4}{l_3}, \frac{ky_4}{l_3}\right] p_1(-\mu_2 x_4 + \alpha_2 l_2 \cos\theta, -\mu_2 y_4) \times \\
 &\times \left. \exp i\varphi_2(-\mu_2 x_4 + \alpha_2 l_2 \cos\theta, -\mu_2 y_4) \otimes P_2(x_4, y_4) \right\}. \quad (13)
 \end{aligned}$$

The physical meaning of this result is that the diameter of the aperture diaphragm does not exceed the interference bandwidth for the interference pattern localized in the hologram plane, so that the two speckle fields from the two exposures are correlated behind the diaphragm.

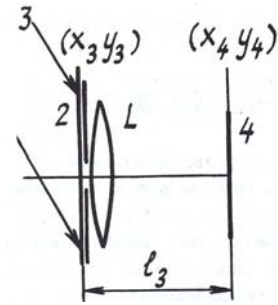


FIG. 3. Spatial filtration of the light field of a doubly exposed hologram in the minus-first order of diffraction in the image plane of the mat screen.

As follows from Eq. (13), the correlating speckle fields from the two exposures coincide in the detection plane 4 within the range of the overlapping images of the pupil of lens L_1 . Therefore the interference pattern characterizing the wave aberrations produced by the lens L_1 is localized in the (x_4, y_4) plane. Indeed, if the period of the function

$$\exp i[\varphi_2(-\mu_2 x_4 + \alpha_2 l_2 \cos\theta, -\mu_2 y_4) - \varphi_2(-\mu_2 y_4)]$$

exceeds the size of the speckle in the detection plane by at least one order of magnitude (the latter determined by the width of the function $P_2(x_4, y_4)$), that function may be taken out of the convolution integral in expression (13). The irradiance distribution in the (x_4, y_4) plane is then given by

$$\begin{aligned}
 I(x_4, y_4) &\sim \left\{ 1 + \cos\left[\varphi_2(-\mu_2 x_4 + \alpha_2 l_2 \cos\theta, -\mu_2 y_4) - \right. \right. \\
 &\left. \left. - \varphi_2(-\mu_2 x_4, -\mu_2 y_4)\right] \right\} \left| F\left[\frac{kx_4}{l_3}, \frac{ky_4}{l_3}\right] \otimes P_2(x_4, y_4) \right|^2, \quad (14)
 \end{aligned}$$

which describes the speckle structure modulated by the interference bands. The interference pattern then presents a shear interferogram in the bands of infinite width, characterizing the axial wave aberrations by lens L_1 .

In contrast to the presentation given in Ref. 1, the photographic plate records subjective speckles described by expressions (2) and (3) (see Fig. 1). Consider a small spatial element of the image of the mat screen, its center coincident with the optical axis. Note that the distribution of the complex amplitude of the field within each individual speckle results from diffraction of a divergent spherical wave at the aperture of lens L_1 . This wave comes from the corresponding points in the object plane, located close to the optical axis. Now let the aperture diaphragm p_2 be shifted in the direction of the x axis in the (x_3, y_3) plane. Let the speckle be identical within the diameter of the aperture diaphragm, and the complex amplitude distribution within each speckle result from the diffraction of a divergent spherical wave coming from the corresponding points in the object plane. It follows

from Ref. 5 that the interference pattern in the detection plane 4 (Fig. 1) will then present a shear interferogram in bands of infinite width, and that the interferogram will characterize the combined on-axis and off-axis wave aberrations due to the lens L_1 . Now we perform spatial filtration in the (x_4, y_4) plane (see Figs. 1, 2) aimed at separating the two shear interferograms: one characterizing the phase distortions of the mat screen wavefront, and the other characterizing the phase distortions of the reference wavefront. Apparently, the displacement p_3 of the diaphragm of the optical axis along the x axis will then result in an alteration of the interference pattern because the lens L_1 introduces off-axis wave aberrations into the overall picture. Besides, for the same reasons, such spatial filtration in the hologram plane is necessary if $\varphi_1(x_1, y_1) = \varphi_3(x_3, y_3) = 0$.

The range of control of the lens L_1 over the field is limited by the resolution ν_0 of the holographic medium and by its physical dimensions. For example, to observe the interference pattern within the total pupil of lens L_1 , the diameter of the illuminated zone of the mat screen D must satisfy the condition $D \geq d/\mu_1$, where d is the pupil diameter (for $\mu_1 \leq 1$), or $D \geq d$ (for $\mu_1 \geq 1$). In addition, the maximum spatial frequency ν_m is given by the expression

$$\frac{1}{\lambda} \sin \left[\theta + \arctg \left[(\mu_1 D + d) / 2l_2 \right] \right]$$

where λ is the wavelength of the coherent source used to record and reproduce the hologram. To spatially separate the holographically reproduced fields in the zeroth and plus and minus first diffraction orders, it is necessary that $\theta \geq 3 \arctg \left[(\mu_1 D + d) / 2l_2 \right]$. The condition $\nu_m \leq \nu_0$ then describes the range of control of lens L_1 over the field for the given dimensions of the recording medium.

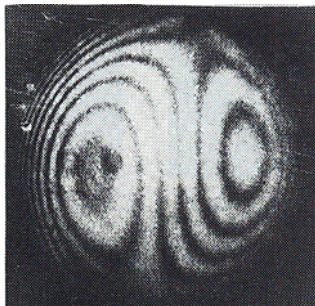


FIG. 4. Shear interferogram characterizing the aberration of the mat screen wavefront and the reference wavefront.

During the actual experiment the doubly exposed holograms were recorded on the Makrat VRL photographic plates. The required illumination was produced by a He-Ne laser ($\lambda = 0.63 \mu\text{m}$). The controllable lenses were of 100–160 mm focal length and 15–30 mm diameter. The experimentally obtained results, which support our theoretical estimates, may be illustrated by considering, by way of example, a

lens of $f_1 = 120$ mm focal length, 30 mm diameter, which served to record the holograms of the focused image of the mat screen at unit magnification. The diameter illuminated spot on the screen was 50 mm. The angles θ and $\alpha_1 = \alpha_2$ were respectively $12^\circ \pm 20'$, and $11'30'' \pm 2''$. Figure 4 shows the shear interferogram, which primarily characterizes the spatial aberration due to transfocal defocusing of the mat screen wavefront and of the reference wavefront, which was recorded during spatial filtration on the optical axis in the image plane of the pupil of lens L_1 (see Fig. 1). Spatial filtration in the hologram plane was performed by recovering the hologram using an unopened laser beam of approximately 2 mm diameter. Figure 5a shows such a shear interferogram, obtained during spatial filtration on the optical axis. The interference pattern characterizes the spherical aberration resulting from transfocal defocusing by the lens L_1 . Figure 5b presents another shear interferogram, obtained by spatial filtration on the x axis, at an edge point of the screen image ($x_{3,0} = 25$ mm). According to Ref. 6 the corresponding interference pattern combines on-axis (Fig. 5a) with off-axis aberrations (Fig. 5b).

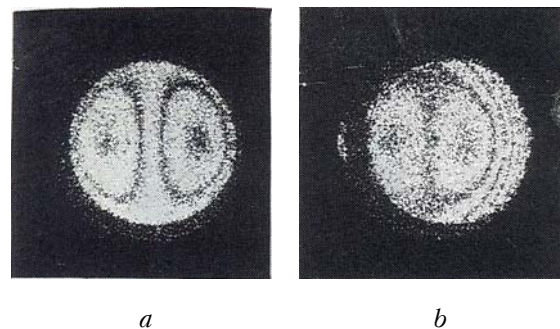


FIG. 5. Shear interferograms characterizing the wave aberrations of the controllable lens L_1 recorded while conducting the spatial filtration in the hologram plane: a — on the optical axis; b — off the optical axis on the edge of the mat screen image.

It follows from Eq. (5) that if the phase change $\varphi_2(-\mu_2 x_4, -\mu_2 y_4) - \varphi_2(-\mu_2 x_4 + \alpha_2 l_2 \cos \theta, -\mu_2 y_4)$ within the image of the pupil of lens I, does not exceed π , then the interference pattern, which combines phase distortions of the illuminating and the reference wavefronts, maybe recovered without any spatial filtration. By way of an example, consider Fig. 6: the interference pattern in Fig. 6b (for the lens pupil of 3 mm diameter, Fig. 6a) was recovered without such spatial filtration. The corresponding shear interferogram mainly describes the spherical aberration resulting from prefocal defocusing of the illuminating and reference wavefronts. Prefocal defocusing was achieved by inverting the sign of their major radii of curvature prior to recording the double-exposure hologram.

In conclusion, note that in comparison with other well-known techniques of holographic interferometry (see Refs. 6 and 7) the considered technique of shear

hologram recording and filtering of the focused image of mat screen possesses a higher level of information content, making possible the quality control of lenses and objectives by their image fields from just one single hologram. Moreover, these Interference pattern are not affected by the possible low optical quality of the interferometer elements used.

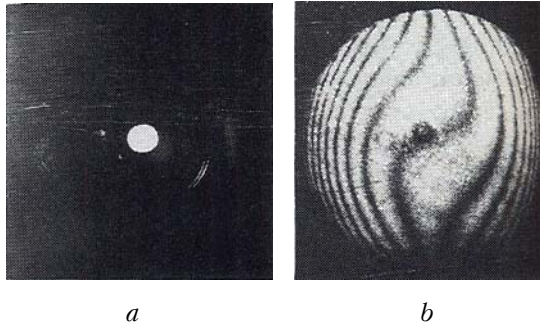


FIG. 6. Irradiance distribution for a small-diameter aperture diaphragm in the plane of lens L_1 (a), in the hologram plane (b).

REFERENCES

1. V.G. Gusev, *Opt. Spektrosk.* **66**, No. 4, 921–924 (1989).
2. J.W. Goodman, *Introduction to Fourier Optics* (McGraw-Hill, New York, 1968).
3. I.S. Klimenko, *Holography of Focused Images and Speckle Interferometry* (Mir, Moscow (1985).
4. R. Jones and C. Wikes, *Holography and Speckle Interferometry*, 2nd ed. (Cambridge Univ. Press, New York, 1989).
5. M. Born and E. Wolf, *Principles of Optics* (Pergamon, Oxford, 1970).
6. D. Malacara, ed., *Optical Shop Testing* (Wiley, New York, 1978).
7. A.K. Beketova, A.F. Belosyrov, A.N. Beryozkin et al., *Holographic Interferometry of Phase Objects* (Nauka, Leningrad, 1979).